Submitted to ADVANCED MATERIALS

Zn-Ion Hybrid Micro-Supercapacitors with Ultrahigh Areal Energy Density and Long-Term Durability

Panpan Zhang, Yang Li, Gang Wang, Faxing Wang, Sheng Yang, Feng Zhu, Xiaodong Zhuang, Oliver G. Schmidt, Xinliang Feng

Advanced Materials, **2019**, Volume 31, Issue 3, 1806005

which has been published in final form at https://doi.org/10.1002/adma.201806005.

Submitted to ADVANCED MATERIALS
DOI: 10.1002/adma.((please add manuscript number))
Article type: Communication

Zn-Ion Hybrid Microsupercapacitors with Ultrahigh Areal Energy Density and Long-Term Durability

By *Panpan Zhang, Yang Li, Gang Wang, Faxing Wang, Sheng Yang, Feng Zhu*, Xiaodong Zhuang, Oliver G. Schmidt, and Xinliang Feng**

P. Zhang, F. Wang, Dr. G. Wang, Dr. S. Yang, Prof. X. Zhuang, Prof. X. Feng
Faculty of Chemistry and Food Chemistry, School of Science, Technische Universität Dresden, Mommsenstr. 4, 01069 Dresden, Germany.
E-mail: xinliang.feng@tu-dresden.de
P. Zhang, F. Wang, Dr. G. Wang, Dr. S. Yang, Prof. X. Zhuang, Prof. O. G. Schmidt, Prof. X. Feng
Center for Advancing Electronics Dresden (cfaed), Technische Universität Dresden, 01062 Dresden, Germany.
Y. Li, Dr. F. Zhu, Prof. O. G. Schmidt
Material Systems for Nanoelectronics, Chemnitz University of Technology, Reichenhainer Str. 70, 09107 Chemnitz, Germany.
Y. Li, Dr. F. Zhu, Prof. O. G. Schmidt
Institute for Integrative Nanosciences, IFW Dresden, 01069 Dresden, Germany.
E-mail: f.zhu@ifw-dresden.de
Prof. X. Zhuang, Prof. X. Feng
The State Key Laboratory of Metal Matrix Composites & Shanghai Key Laboratory of Electrical Insulation and Thermal Ageing, School of Chemistry and Chemical Engineering, Shanghai Jiao Tong University, Dongchuan Road 800, 200240 Shanghai, China.

Keywords: Zn-ion, hybrid microsupercapacitor, energy density, durability

Abstract: On-chip microsupercapacitors (MSCs), as promising power candidates for micro-devices, typically exhibit high power density, large charge/discharge rates, and long cycling lifetimes. However, as for most reported MSCs, the unsatisfied areal energy density (<10 μWh cm^{-2}) still hinder their practical applications. Herein, a new-

type Zn-ion hybrid MSC with ultrahigh areal energy density and long-term durability is demonstrated. Benefiting from fast ion adsorption/desorption on the capacitor-type activated carbon cathode and reversible Zn stripping/plating on the battery-type electrodeposited Zn nanosheets anode, the fabricated Zn-ion hybrid MSCs exhibit remarkable areal capacitance of 1297 mF cm^{-2} at 0.16 mA cm^{-2}, landmark areal energy density (115.4 μWh cm^{-2} at 0.16 mW cm^{-2}), as well as a superb cycling stability without noticeable decay after 10000 cycles. This work will inspire the fabrication and development of new high-performance micro-energy devices based on novel device design.

Nowadays, the development of portable and implantable electronics has focused on the miniaturization, long-term, and high-speed operation, thus further stimulating the enormous demand for high-performance miniaturized energy storage devices (MESDs).[1] Among those MESDs, the emerging in-plane microsupercapacitors (MSCs) have been regarded as one promising power sources owing to their ultrahigh power densities, fast rate capabilities, and excellent cycle lifetimes.[2] So far, a variety of active materials, such as graphene-based materials,[3] transition metal oxides,[4] hydroxides,[5] and dichalcogenides,[6] MXenes,[7] and conducting polymers,[8] have been developed to achieve good overall electrochemical performance. Due to the limited occupied area of MSCs in on-chip electronics, the performance should be calculated based on area rather than by volume or mass.[2a, 9] However, most reported

MSCs mentioned above still suffered from the unsatisfied areal energy densities (<10 μWh cm^{-2}), which hindered their practical applications.

In general, supercapacitors (SCs) provide fast charge/discharge capability (high power density) because of surface-mediated ion diffusion. Rechargeable batteries (RBs) rely on the reversible redox reaction on the surface of active materials in the bulk form for charge storage.[10] As a result, RBs have much higher specific energy densities, but they generally exhibit insufficient power densities ascribing to slow ion diffusion rates in solid electrode materials. Therefore, constructing a hybrid supercapacitor with a battery-type anode electrode and a capacitor-type cathode electrode has been an attractive strategy to gain the merits from both RBs and SCs.[11] In this respect, hybrid SCs based on both of monovalent cations[12] (Li^+, Na^+, K^+) and multivalent cations[13] (Mg^{2+}, Zn^{2+}, Ni^{2+}, Ca^{2+}, Al^{3+}) have been considered as research hotspots. Compared to the monovalent cation-based SCs, multivalent devices are less sensitive to the air and can be more suitable for practical applications. Despite these merits and great research interests, the study on multivalent ion-based in-plane MSCs for on-chip electronics has not been reported yet.

Herein, we demonstrate a new-type Zn-ion hybrid MSC with ultrahigh areal energy density and long-term durability by employing activated carbon (AC) as a cathode and electrodeposited Zn nanosheets as an anode in $ZnSO_4$ based aqueous electrolyte. Fast ion adsorption/desorption on the AC cathode and reversible Zn stripping/plating on the electrodeposited Zn nanosheets anode enable the Zn-ion hybrid MSCs to achieve a high

charge/discharge capability. As a result, the areal capacitance reaches a record of over 1200 mF cm^{-2} at 0.16 mA cm^{-2} in a voltage range of 0.5-1.5 V and the areal energy density of up to 115.4 μWh cm^{-2} at a power density of 0.16 mW cm^{-2}, which are superior to those of the state-of-the-art MSCs. Moreover, the Zn-ion hybrid MSCs exhibit a superb cycling stability without noticeable decay after 10000 cycles. Thereby, the Zn-ion hybrid MSCs with unique characteristics of such excellent reversible capacitance, high-rate capability, and good cycling performance are expected to act as a new generation MESDs.

The whole device fabrication process towards Zn-ion hybrid MSCs is schematically illustrated in **Figure 1**a. First, gold interdigital current collectors were patterned on the clean silicon wafer. Then, 500-μm-thick photoresist frames were built between and around fingers, serving as the mechanical supporter and physical barrier (Figure S1). After that, the Zn nanosheets were electrodeposited on the left gold interdigital fingers with a constant current density to use as the anode electrode. In addition, the slurry consisting of active materials (AC), binder (sodium carboxymethylcellulose, CMC), and conductive additive (acetylene black) was injected into the right trenches for several times to fill the space as the cathode electrode. The different side-view images display the asymmetric configuration (Figure S2). Finally, 2 M $ZnSO_4$ aqueous electrolyte was drop-coated onto the interdigital patterned area and packaged with polyimide film with the help of UV-curing optical adhesive. The devices before and after packaging are depicted in Figure 1b with the total size of 1.8 × 1.8 cm^2. The

fabrication of Zn-ion hybrid MSCs is economic, simple, highly efficient, and compatible with modern silicon-based technology.

The morphologies and structure of electrodeposited Zn nanosheets anode were inspected by scanning electron microscope (SEM), atomic force microscopy (AFM), high-resolution transmission electron microscope (HRTEM), and X-ray diffraction (XRD). The SEM images present that the vertical Zn nanosheets were homogeneously grown on the surface of gold interdigital fingers at a constant current (**Figure 2**a and Figure S3, S4). Additionally, the corresponding AFM images and height profiles imply that the grown Zn nanosheets own lateral dimension of 100-500 nm and average thickness of 5.6 nm (Figure 2b,c). As shown in Figure 2d,e, the HRTEM images and selected area electron diffraction (SAED) pattern confirmed the distinct crystal lattice and atomic structure of Zn nanosheets. The well-defined lattice space of 0.25 nm was observed (Figure 2e), corresponding to the (002) plane of hexagonal zinc (JCPDS: 87-0713).[14] Furthermore, to determine the growth process, various Zn nanosheets samples at different electrodeposition times were investigated with XRD patterns and SEM measurements. All the diffraction peaks were well in accordance with hexagonal zinc (Figure 2f).[14] The discussions of the growth mechanism can be found in Supporting Information, associated with Figure S5. After the electrodeposition of 30 min, the side-view SEM image and corresponding EDS mapping indicate that the thickness of Zn anode in MSCs is around 50 μm (Figure S6). As the positive electrode material, commercial AC was derived from coconut shells and characterized by SEM, HRTEM,

XRD pattern, and Raman spectrum (Figure S7-S9). The specific surface area is as high as 1825 $m^2 g^{-1}$ (Figure S10), beneficial to the sufficient ion adsorption/desorption. After filling the channels by controlled injector for several times, the thickness of AC cathode in MSCs is around 80 μm (Figure S11).

Before assembling the Zn-ion hybrid MSCs, the electrochemical behavior of the Zn nanosheets anode and the AC cathode were firstly investigated by cyclic voltammetry (CV) measurement. As depicted in **Figure 3**a, in the case of the Zn anode, there is one set of redox peaks located at -0.9/-1.2 V (*vs.* SCE), corresponding to the stripping/plating process of Zn/Zn^{2+}. Moreover, the intimate contact between electrodeposited Zn nanosheets anode and aqueous electrolyte guarantees a stable ion transport, as verified by the continuous Zn stripping/plating process (Figure S12). In addition, perfect rectangular CV curves of AC cathode are observed due to the formation of electrochemical double layers (Figure S13). Since there is a wide potential difference (1 V) between Zn and AC, they can be assembled into a Zn-ion hybrid MSC system whose reactions during the charging and discharging processes can be schematically illustrated in Figure 1c. The CV curves of the Zn-ion hybrid MSC at various scan rates between 0.2 and 5 mV s^{-1} (Figure 3b) display the nearly rectangular shape in a potential window of 0.5-1.5 V, illustrating the characteristics of electrochemical double-layer capacitor and also surface redox reactions. Furthermore, the capacitive behavior of the Zn-ion hybrid MSC was investigated through galvanostatic charge-discharge (GCD) measurements at current densities from 0.16 to

3.12 mA cm^{-2} (Figure 3c). According to the GCD curves, the Zn-ion hybrid MSCs delivered an outstanding areal capacitance of 1297 mF cm^{-2} at a current density of 0.16 mA cm^{-2}, which was 10 times higher than that of MnO_2-based MSCs, and much higher than those of graphene-based MSCs and recently reported porous carbon-based MSCs (1-500 mF cm^{-2}, Table S1). Moreover, the areal capacitance retained more than 600 mF cm^{-2} at the high current density of 3.12 mA cm^{-2}. In addition, the Zn-ion hybrid MSC exhibited a superior cycling stability with 100% of capacitance retention after 10000 charge/discharge cycles at 1.56 mA cm^{-2} (Figure 3e). Figure 3f shows the electrochemical impedance spectra (EIS) of Zn-ion hybrid MSCs before and after the cycling measurement. The semicircles in high frequency regions denote charge transfer resistance (R_{ct}), which is related to reaction kinetics, and the slope in low frequency regions represents Zn^{2+} diffusion resistance in the electrolyte. After cycling test, R_{ct} becomes much smaller (114.4 *vs.* 142.5 Ω), suggesting fast reaction kinetics of Zn-ion hybrid MSCs.[4h, 8d]

As the whole device space is greatly concerned in designing MESDs, the areal energy and power densities are more meaningful than those calculated based on mass or volume. Thus, to further demonstrate the overall performance of the Zn-ion hybrid MSCs, Ragone plots were presented in Figure 3g. Notably, our Zn-ion hybrid MSCs delivered an ultrahigh areal energy density of up to 115.4 μWh cm^{-2} at 0.16 mW cm^{-2}, which was much higher than those of recently reported graphene-based MSCs,[3b, 3c, 3f, 4h] polyaniline nanowire MSCs,[15] onion-like carbon MSCs,[3k] activated carbon

MSCs,[3k] and even superior to carbide-derived carbon MSCs[3l] and graphene/MnO_2 MSCs[4d] (0.1-50 μWh cm^{-2}). In addition, Zn-ion hybrid MSC also provided high power density of 3.9 mW cm^{-2} at 89 μWh cm^{-2}, which is superior to that of carbon-based MSCs.[3b, 3c, 3f] As depicted in Table S1, these results for Zn-ion hybrid MSCs are comparable with microbatteries and electrolytic capacitors. In order to achieve higher specific voltage and capacitance, individual units are connected in series and parallel for practical applications. For example, three Zn-ion hybrid MSCs connected in series can reach a high voltage of 4.5 V (Figure S15). Two serially-connected Zn-ion hybrid MSCs can light three characters, "TUD", composed of 33 red LEDs (Figure 3h). Furthermore, two and three Zn-ion hybrid MSCs in a parallel configuration exhibit an enhanced capacitance compared with that of a single one.

In order to study the energy storage mechanisms of Zn nanosheets anode and AC cathode in Zn-ion hybrid MSCs, the XRD patterns at various charge/discharge voltages after the 50th cycle are compared in **Figure 4**a,b. The GCD measurement of Zn-ion hybrid MSCs started at 1.5 V, and then discharged to 0.5 V, finally charged to 1.5 V again. As clearly revealed in Figure 4a, there exist eight main characteristic peaks of (002), (100), (101), (102), (103), (004), (112), and (201) at 2θ of 36.2°, 38.9°, 43.1°, 54.5°, 70.3°, 77.0°, 82.1°, and 86.6°, respectively, for all the Zn nanosheets anodes. As the discharge process advances, the diffraction intensities of both (002) and (004) facets decrease, accompanied by the increase of that of (101) facet, indicating the change of the crystal reorientation during the stripping conversion of Zn nanosheets. Notably, no

other new peaks ascribed to such as ZnO particles can be identified, manifesting the good reversible capability. Conversely, as the charge process continues, the (101) facet gradually vanishes, associated with the recovery of (002) and (004) facets. In addition, as displayed in Figure 4c and Figure S16, Zn anode still exhibits the nanosheet morphology after cycling measurement. The absence of ZnO is due to the neutral electrolyte, which does not result in the formation of $Zn(OH)_2$.[16] In addition, the vertical nanosheets with porous structure hinder the seed growth of Zn dendrite. These results suggest the Zn stripping/plating with excellent reversibility on the Zn nanosheets anode. The structural change at the AC cathode was also examined with XRD and SEM investigations. During the GCD process, the location and intensity of (002) peak remained unchanged, indicating a physical adsorption/desorption process. Also, the morphology of AC cathode after cycling testing (Figure 4d and Figure S17) did not show obvious variation. All these results support the good cycling stability of Zn-ion hybrid MSCs at both low and high current densities.

In summary, we demonstrate a novel Zn-ion hybrid MSC by using electrodeposited Zn nanosheets anode and AC cathode in an aqueous electrolyte. The fabricated Zn-ion hybrid MSCs exhibit ultrahigh areal capacitance of 1297 mF cm^{-2} at 0.16 mA cm^{-2}, landmark areal energy density (115.4 μWh cm^{-2} at 0.16 mW cm^{-2}), as well as long lifetime, thanks to the hybrid device structure with a battery-type anode and a capacitor-type cathode. We believe that this study not only provides new ideas for developing

high-performance MSCs, but also shows potential perspective for the integration in miniaturized intelligent electronics.

Supporting Information

Supporting Information is available online from the Wiley Online Library or from the author.

Acknowledgements

P.Z. and Y.L. contributed equally to this work. The authors thank the financial support from the German Research Foundation (DFG) within the Cluster of Excellence 'Center for Advancing Electronics Dresden' (cfaed) and financed by the Initiative and Networking Fund of the German Helmholtz Association, Helmholtz International Research School for Nanoelectronic Networks NanoNet (VH-KO-606), Hamburg Science Award, ERC Grant on 2DMATER, HIPER-G, NSFC (21720102002, 51722304), and EU Graphene Flagship. The authors thank Dr. Jian Zhang for helpful discussions and Dr. Lanlan Wang (Xi'an Jiaotong University) for her assistance in materials measurements. We acknowledge the use of the facilities in the Dresden Center for Nanoanalysis at the Technische Universität Dresden.

Received: ((will be filled in by the editorial staff))
Revised: ((will be filled in by the editorial staff))
Published online: ((will be filled in by the editorial staff))

[1] a) F. Yi, H. Ren, J. Shan, X. Sun, D. Wei, Z. Liu, *Chem. Soc. Rev.* **2018**, *47*, 3152; b) D. P. Dubal, N. R. Chodankar, D. H. Kim, P. Gomez-Romero, *Chem. Soc. Rev.* **2018**, *47*, 2065; c) Z. Lou, Li, L. Wang, G. Shen, *Small* **2017**, *13*, 1701791; d) P. Zhang, F. Wang, M. Yu, X. Zhuang, X. Feng, *Chem. Soc. Rev.* **2018**, DOI: 10.1039/C8CS00561C; e) D. Yu, K. Goh, H. Wang, L. Wei, W. Jiang, Q. Zhang, L. Dai, Y. Chen, *Nat. Nanotechnol.* **2014**, *9*, 555.

[2] a) N. A. Kyeremateng, T. Brousse, D. Pech, *Nat. Nanotechnol.* **2017**, *12*, 7; b) D. Qi, Y. Liu, Z. Liu, L. Zhang, X. Chen, *Adv. Mater.* **2017**, *29*, 1602802.

[3] a) L. Wei, N. Nitta, G. Yushin, *ACS Nano* **2013**, *7*, 6498; b) M. Beidaghi, C. Wang, *Adv. Funct. Mater.* **2012**, *22*, 4501; c) J. Lin, C. Zhang, Z. Yan, Y. Zhu, Z. Peng, R. H. Hauge, D. Natelson, J. M. Tour, *Nano Lett.* **2013**, *13*, 72; d) G. Lee, D. Kim, D. Kim, S. Oh, J. Yun, J. Kim, S.-S. Lee, J. S. Ha, *Energy Environ. Sci.* **2015**, *8*, 1764; e) S.-K. Kim, H.-J. Koo, A. Lee, P. V. Braun, *Adv. Mater.* **2014**, *26*, 5108; f) M. F. El-Kady, R. B. Kaner, *Nat. Commun.* **2013**, *4*, 1475; g) Z. S. Wu, K. Parvez, X. Feng, K. Müllen, *Nat. Commun.* **2013**, *4*, 2487; h) J. Lin, Z. Peng, Y. Liu, F. Ruiz-Zepeda, R. Ye, E. L. Samuel, M. J. Yacaman, B. I. Yakobson, J. M. Tour, *Nat. Commun.* **2014**, *5*, 5714; i) W. Gao, N. Singh, L. Song, Z. Liu, A. L. M. Reddy, L. Ci, R. Vajtai, Q. Zhang, B. Wei, P. M. Ajayan, *Nat. Nanotechnol.* **2011**, *6*, 496; j) D. Qi, Z. Liu, Y. Liu, W. R. Leow, B. Zhu, H. Yang, J. Yu, W. Wang, H. Wang,

S. Yin, X. Chen, *Adv. Mater.* **2015**, *27*, 5559; k) D. Pech, M. Brunet, H. Durou, P. Huang, V. Mochalin, Y. Gogotsi, P.-L. Taberna, P. Simon, *Nat. Nanotechnol.* **2010**, *5*, 651; l) P. Huang, C. Lethien, S. Pinaud, K. Brousse, R. Laloo, V. Turq, M. Respaud, A. Demortière, B. Daffos, P. L. Taberna, B. Chaudret, Y. Gogotsi, P. Simon, *Science* **2016**, *351*, 691.

[4] a) A. Ferris, S. Garbarino, D. Guay, D. Pech, *Adv. Mater.* **2015**, *27*, 6625; b) Y.-Q. Li, X.-M. Shi, X.-Y. Lang, Z. Wen, J.-C. Li, Q. Jiang, *Adv. Funct. Mater.* **2016**, *26*, 1830; c) Y. Lin, Y. Gao, Z. Fan, *Adv. Mater.* **2017**, *29*, 1701736; d) M. F. El-Kady, M. Ihns, M. Li, J. Y. Hwang, M. F. Mousavi, L. Chaney, A. T. Lech, R. B. Kaner, *Proc. Natl. Acad. Sci. USA* **2015**, *112*, 4233; e) J. Han, Y.-C. Lin, L. Chen, Y.-C. Tsai, Y. Ito, X. Guo, A. Hirata, T. Fujita, M. Esashi, T. Gessner, M. Chen, *Adv. Sci.* **2015**, *2*, 1500067; f) X. Wang, B. D. Myers, J. Yan, G. Shekhawat, V. Dravid, P. S. Lee, *Nanoscale* **2013**, *5*, 4119; g) Y. Yue, Z. Yang, N. Liu, W. Liu, H. Zhang, Y. Ma, C. Yang, J. Su, L. Li, F. Long, Z. Zou, Y. Gao, *ACS Nano* **2016**, *10*, 11249; h) P. Zhang, F. Zhu, F. Wang, J. Wang, R. Dong, X. Zhuang, O. G. Schmidt, X. Feng, *Adv. Mater.* **2017**, *29*, 1604491; i) D. Kim, J. Yun, G. Lee, J. S. Ha, *Nanoscale* **2014**, *6*, 12034.

[5] a) N. Kurra, N. A. Alhebshi, H. N. Alshareef, *Adv. Energy Mater.* **2015**, *5*, 1401303; b) H. Wu, K. Jiang, S. Gu, H. Yang, Z. Lou, D. Chen, G. Shen, *Nano Res.* **2015**, *8*, 3544; c) N. Kurra, Q. Jiang, H. N. Alshareef, *Nano Energy* **2015**, *16*, 1.

[6] a) W. Yang, L. He, X. C. Tian, M. Y. Yan, H. Yuan, X. B. Liao, J. S. Meng, Z. M. Hao, L. Q. Mai, *Small* **2017**, *13*, 1700639; b) J. Feng, X. Sun, C. Wu, L. Peng, C. Lin, S. Hu, J. Yang, Y. Xie, *J. Am. Chem. Soc.* **2011**, *133*, 17832; c) J. Wu, J. Peng, Z. Yu, Y. Zhou, Y. Guo, Z. Li, Y. Lin, K. Ruan, C. Wu, Y. Xie, *J. Am. Chem. Soc.* **2018**, *140*, 493.

[7] N. Kurra, B. Ahmed, Y. Gogotsi, H. N. Alshareef, *Adv. Energy Mater.* **2016**, *6*, 1601372.

[8] a) Z. S. Wu, K. Parvez, S. Li, S. Yang, Z. Liu, S. Liu, X. Feng, K. Müllen, *Adv. Mater.* **2015**, *27*, 4054; b) M. Zhu, Y. Huang, Y. Huang, H. Li, Z. Wang, Z. Pei, Q. Xue, H. Geng, C. Zhi, *Adv. Mater.* **2017**, *29*, 1605137; c) R. S. Guo, J. T. Chen, B. J. Yang, L. Y. Liu, L. J. Su, B. S. Shen, X. B. Yan, *Adv. Funct. Mater.* **2017**, *27*, 1702394; d) P. Zhang, J. Wang, W. Sheng, F. Wang, J. Zhang, F. Zhu, X. Zhuang, R. Jordan, O. G. Schmidt, X. Feng, *Energy Environ. Sci.* **2018**, *11*, 1717; e) C. Z. Meng, J. Maeng, S. W. M. John, P. P. Irazoqui, *Adv. Energy Mater.* **2014**, *4*, 1301269.

[9] M. Beidaghi, Y. Gogotsi, *Energy Environ. Sci.* **2014**, *7*, 867.

[10] a) J. Jiang, Y. Li, J. Liu, X. Huang, C. Yuan, X. W. Lou, *Adv. Mater.* **2012**, *24*, 5166; b) J. W. Choi, D. Aurbach, *Nat. Rev. Mater.* **2016**, *1*, 16013.

[11] a) D. P. Dubal, O. Ayyad, V. Ruiz, P. Gomez-Romero, *Chem. Soc. Rev.* **2015**, *44*, 1777; b) M. R. Lukatskaya, B. Dunn, Y. Gogotsi, *Nat. Commun.* **2016**, *7*, 12647; c) N. Choudhary, C. Li, J. Moore, N. Nagaiah, L. Zhai, Y. Jung, J. Thomas, *Adv. Mater.* **2017**, *29*, 1605336.

[12] a) P. Jeżowski, O. Crosnier, E. Deunf, P. Poizot, F. Béguin, T. Brousse, *Nat. Mater.* **2017**, *17*, 167; b) F. Wang, X. Wang, Z. Chang, X. Wu, X. Liu, L. Fu, Y. Zhu, Y. Wu, W. Huang, *Adv. Mater.* **2015**, *27*, 6962; c) P. Zhang, X. Zhao, Z. Liu, F. Wang, Y. Huang, H. Li, Y. Li, J. Wang, Z. Su, G. Wei, Y. Zhu, L. Fu, Y. Wu, W. Huang, *NPG Asia Mater.* **2018**, *10*, 429; d) L. Fan, K. Lin, J. Wang, R. Ma, B. Lu, *Adv. Mater.* **2018**, *30*, 1800804.

[13] a) Z. Li, K. Xiang, W. Xing, W. C. Carter, Y.-M. Chiang, *Adv. Energy Mater.* **2015**, *5*, 1401410; b) F. Wang, Z. Liu, X. Wang, X. Yuan, X. Wu, Y. Zhu, L. Fu, Y. Wu, *J. Mater. Chem. A* **2016**, *4*, 5115; c) H. D. Yoo, S.-D. Han, R. D. Bayliss, A. A. Gewirth, B. Genorio, N. N. Rajput, K. A. Persson, A. K. Burrell, J. Cabana, *ACS Appl. Mater. Interfaces* **2016**, *8*, 30853.

[14] Y. Zeng, X. Zhang, Y. Meng, M. Yu, J. Yi, Y. Wu, X. Lu, Y. Tong, *Adv. Mater.* **2017**, *29*, 1700274.

[15] K. Wang, W. Zou, B. Quan, A. Yu, H. Wu, P. Jiang, Z. Wei, *Adv. Energy Mater.* **2011**, *1*, 1068.

[16] X. Wang, F. Wang, L. Wang, M. Li, Y. Wang, B. Chen, Y. Zhu, L. Fu, L. Zha, L. Zhang, Y. Wu, W. Huang, *Adv. Mater.* **2016**, *28*, 4904.

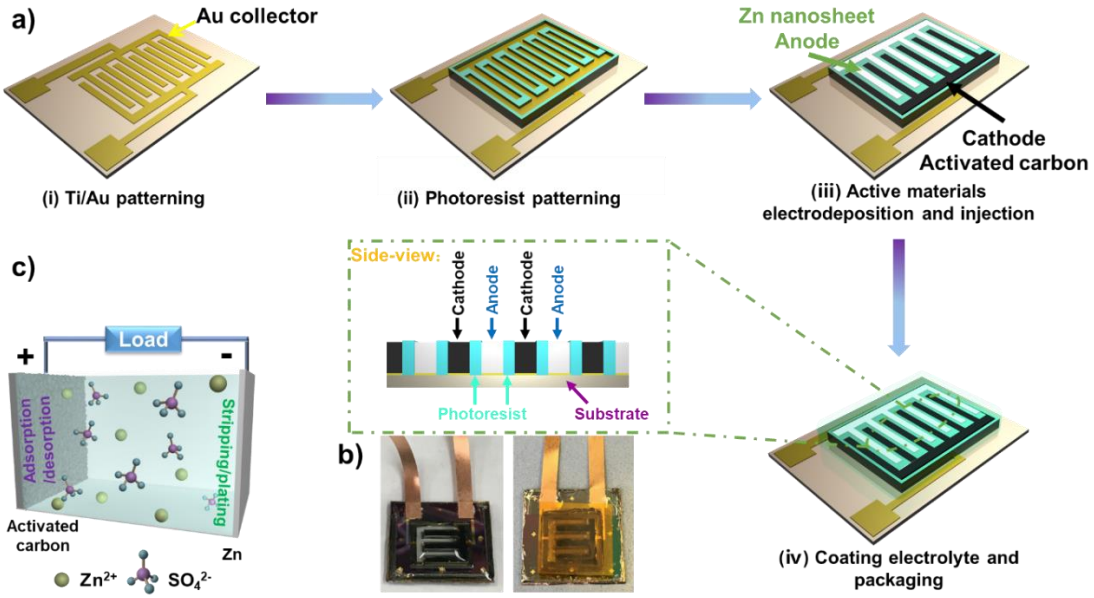

Figure 1. a) Schematic of the fabrication process of Zn-ion hybrid MSCs: (i) patterning gold interdigital current collectors onto the clean substrate; (ii) building photoresist separator between and around the interdigital fingers; (iii) electrodepositing Zn nanosheets as anode material and injecting the slurry containing AC, CMC, and acetylene black as cathode material; (iv) drop-coating aqueous electrolyte and packaging with polyimide film. b) Optical images of Zn-ion hybrid MSCs before and after packaging. c) Mechanism of Zn-ion hybrid MSCs based on simultaneous anion adsorption/desorption on AC cathode electrode and Zn^{2+} stripping/plating on electrodeposited Zn nanosheets anode electrode.

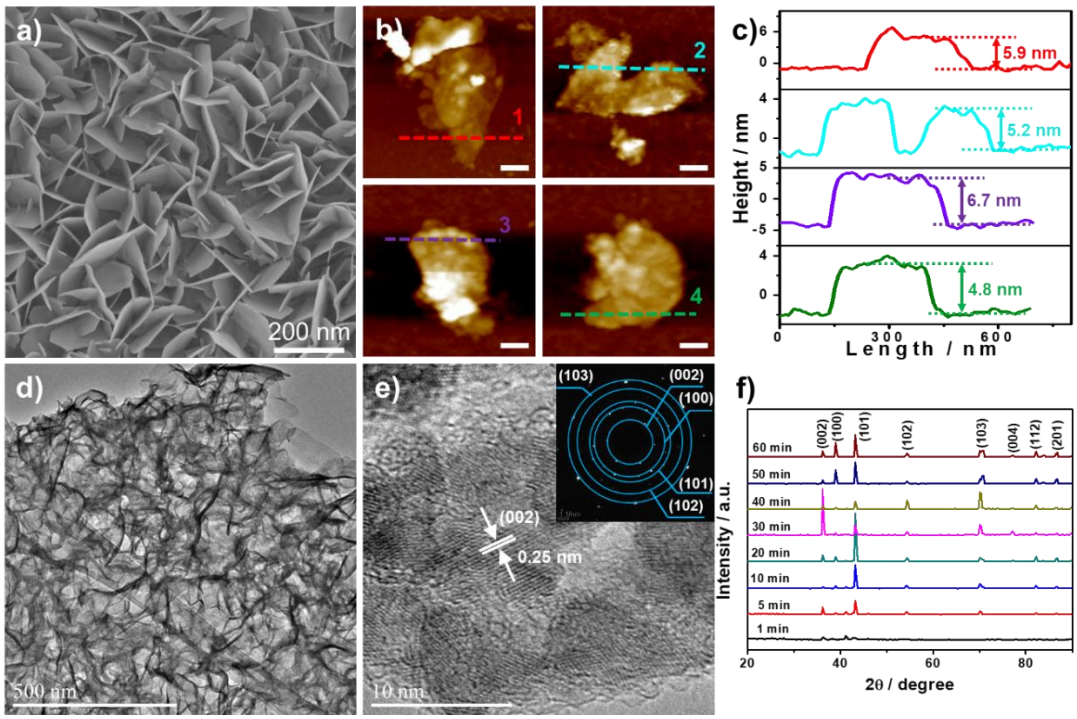

Figure 2. Characterizations of electrodeposited Zn nanosheets as anode materials. a) SEM image of electrodeposited Zn nanosheets. b) AFM images and c) corresponding height profiles of Zn nanosheets; scale bars, 100 nm. d, e) HRTEM images of electrodeposited Zn nanosheets with different magnifications. Inset shows the SAED pattern. f) XRD patterns of Zn nanosheets on the gold interdigital current collectors with different electrodeposition times.

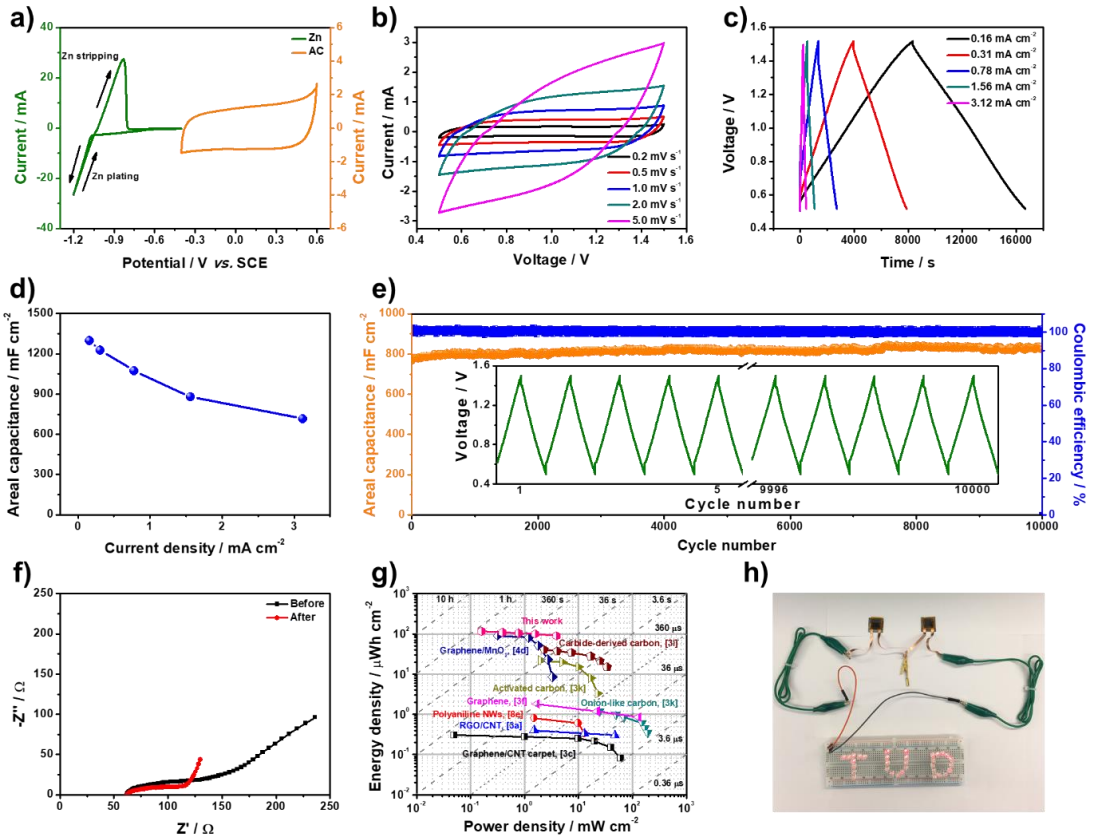

Figure 3. Electrochemical behavior of Zn-ion hybrid MSCs. a) CV curves of the Zn anode and AC cathode in 2 M $ZnSO_4$ aqueous electrolyte at a scan rate of 10 mV s^{-1}. b) CV curves at varies scan rates of 0.2-5 mV s^{-1}. c) GCD curves at different current densities of 0.16-3.12 mA cm^{-2}. d) Areal capacitance calculated from GCD curves as function of current densities. e) Cycling stability at the current density of 1.56 mA cm^{-2}. Inset shows the first five and the last five GCD curves of Zn-ion hybrid MSCs. f) Nyquist plots of the fabricated Zn-ion hybrid MSCs before and after 10000 charge-discharge cycling measurement. g) Ragone plots for Zn-ion hybrid MSCs, carbon-based MSCs, graphene-based MSCs and conducting polymer-based MSCs. h) Photograph of two Zn-ion hybrid MSCs connected in series powering a LED array of "TUD" logo.

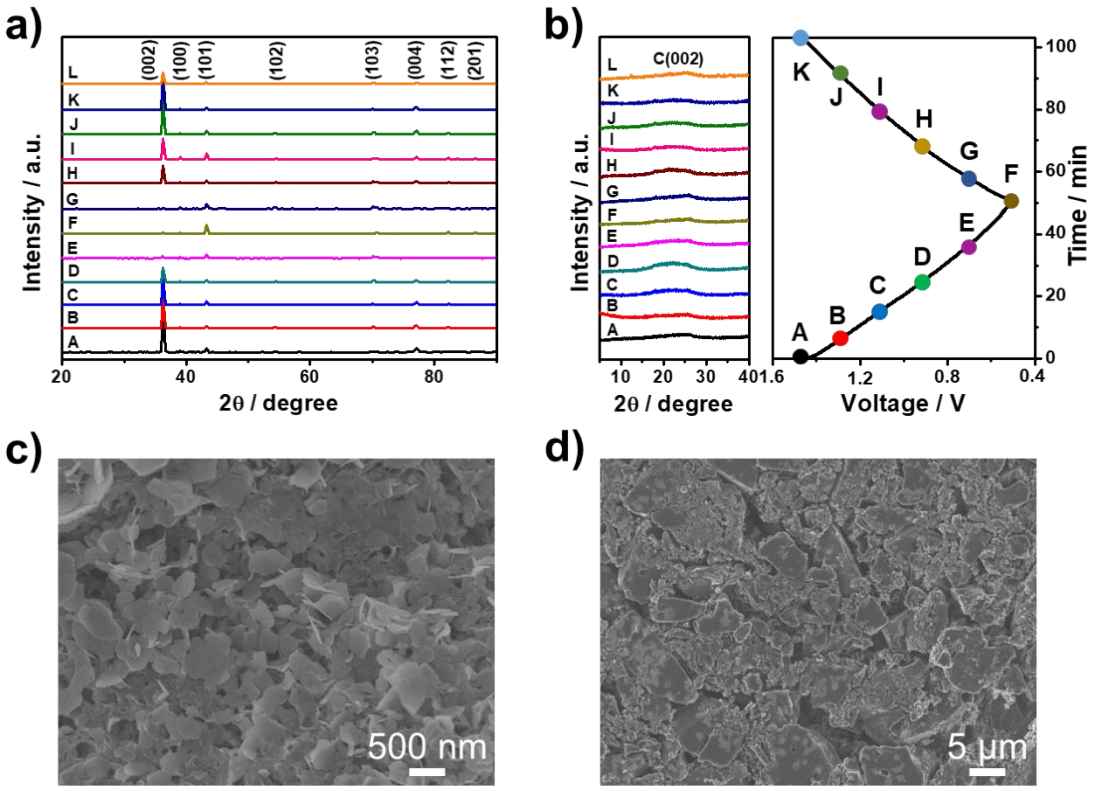

Figure 4. Mechanism study of Zn-ion hybrid MSCs. Ex-situ XRD patterns of a) Zn nanosheets anode and b) AC cathode after the 50th cycle at 0.5 mA cm^{-2} between 0.5 and 1.5 V. The curves L represent the XRD patterns after 10000 cycling testing. SEM images of c) Zn nanosheets anode and d) AC cathode after 10000 cycling measurements.